ISSN 0023-1584, Kinetics and Catalysis, 2007, Vol. 48, No. 1, pp. 136–142. © MAIK "Nauka/Interperiodica" (Russia), 2007.
Original Russian Text © A.A. Lamberov, S.R. Egorova, I.R. Il'yasov, Kh.Kh. Gil'manov, S.V. Trifonov, V.M. Shatilov, A.Sh. Ziyatdinov, 2007, published in Kinetika i Kataliz, 2007, Vol. 48, No. 1, pp. 143–149.

Changes in the Course of Reaction and Regeneration of a Pd–Ag/Al_2O_3 Catalyst for the Selective Hydrogenation of Acetylene

A. A. Lamberov[a], S. R. Egorova[a], I. R. Il'yasov[a], Kh. Kh. Gil'manov[b], S. V. Trifonov[b], V. M. Shatilov[b], and A. Sh. Ziyatdinov[b]

[a] *Kazan State University, Kazan, 420008 Tatarstan, Russia*
E-mail: segorova@rambler.ru
[b] *OAO Nizhnekamskneftekhim, Nizhnekamsk, 423574 Tatarstan, Russia*

Received March 9, 2005

Abstract—The samples of Pd–Ag/Al_2O_3 catalysts for the selective hydrogenation of acetylene impurities in an ethane–ethylene mixture were studied using the IR spectroscopy of adsorbed CO, X-ray diffraction analysis, and thermogravimetry. In the course of reaction and regeneration, the total concentration of the supported metals (Pd and Ag) changed only slightly. The degree of accessibility of silver atoms to CO adsorption and the amount of these atoms in the nearest environment of palladium atoms decreased to result in an increase in the selectivity of acetylene hydrogenation to ethane. The decrease in the accessibility of silver was due to a change in the phase composition of the alumina support as a result of its rehydration. It was hypothesized that the resulting aluminum hydroxide with the boehmite morphology is a source of the strongest Lewis acid sites, which catalyze oligomerization processes on the catalyst surface.

DOI: 10.1134/S0023158407010181

INTRODUCTION

Palladium catalysts are widely used in organic synthesis and petroleum chemistry in hydrogenation, hydrocracking, and flue-gas combustion processes. Supported palladium systems play a special role in the hydrogenation of alkyne impurities in alkenes, for example, at the stages of monomer preparation in the cycles of polymer synthesis [1]. Thus, because of the poisoning effect of acetylene on polymerization catalysts, the concentration of acetylene in ethylene raw materials should be decreased to 10 ppm.

The hydrogenation of acetylene impurities in ethane–ethylene mixtures was performed primarily in the presence of Pd–Al_2O_3 catalysts promoted with Group IB elements [2]. The activity and selectivity of catalysts depend significantly on the properties of the supported metal (the oxidation number, dispersity, and distribution density of palladium particles), as well as on reaction conditions. In the course of operation, the catalyst activity and selectivity decreased because of the deactivation of the active component by oligomer deposits [3]; this decrease was compensated by an increase in the reaction temperature [2].

The deactivation of catalysts for the selective hydrogenation of acetylene in the course of operation has been widely discussed in the scientific literature [3–9]. The primary attention of researchers has been focused on changes in the properties of the active component: the aggregation of its particles, catalyst poisoning, and surface blocking with oligomerization products. In this case, changes in the state of the support and the contribution of the support to the deactivation of the catalytic system have not been taken into consideration in actual practice. Nevertheless, it is well known [7, 8, 10, 11] that the alumina support is not indifferent to supported metals (Pd, Pt, and Ag), and it exerts a noticeable effect on their properties and the degree of interaction with the surface. However, studies on the effects of support transformations on the state of supported metals in catalysts have not been performed.

The aim of this work was to study changes in the activity and selectivity of a catalyst for the selective hydrogenation of acetylene in an ethane–ethylene mixture depending on the phase transformations of the alumina support and to evaluate the effect of support characteristics on the states of the active component and a promoter in the course of reaction and regeneration.

EXPERIMENTAL

The test materials were a fresh sample (sample A) and the samples of a catalyst for the selective hydrogenation of acetylene in an ethane–ethylene mixture after operation under conditions of a commercial process (samples B and C). The catalyst was palladium (0.03 wt %) and silver (0.20 wt %) supported onto the outer surface of spherical aluminum oxide granules 2.5–3.0 mm in diameter. The total operation times were 17000 and 22000 h for samples B and C, respectively.

The intermediate regeneration of the catalyst was performed by successively treating with methane (T = 473 K; P = 0.5 MPa), water vapor (T = 653 K; P = 0.2 MPa), and atmospheric oxygen (T = 713 K; P = 0.3 MPa). The duration of the steam regeneration was ~80 h. The additional oxidative thermal treatment of the samples was performed under laboratory conditions at 673 K for 3 h in an atmosphere of air. The interregeneration cycles of the catalyst varied from ~5000 h at the beginning of operation to ~1000 h at the end.

The catalysts were tested in the reaction of selective acetylene hydrogenation into ethylene in an ethane–ethylene mixture containing 2.13 vol % C_2H_2, 76.41 vol % C_2H_4, and 21.46 vol % C_2H_6. The tests were performed in a laboratory flow-type reactor with a catalyst loading of 7 cm^3 at a space velocity of the ethane–ethylene mixture equal to 2500 h^{-1}, at a pressure of 1 MPa over a reaction temperature range from 293 to 323 K. The temperature in the catalyst bed was monitored with a Chromel–Alumel thermocouple (to within ±1 K); a specified value was maintained using a Sh-0403 thermoregulator. The ethane–ethylene mixture was diluted with hydrogen based on the molar ratio $C_2H_2/H_2 = 1 : 1.4$. The catalysts were reduced in a flow of hydrogen at 403 K for 4 h at a pressure of 0.5 MPa. The concentrations of reactants and reaction products with time were measured by chromatography; based on these data, the activity of catalysts and the selectivity for ethylene and ethane were determined. The catalyst activity in the reaction of acetylene hydrogenation was calculated as the total amount of C_2H_2 reacted in 1-h tests per unit weight of palladium ($A_{C_2H_2}$). The total amount of C_4^{tot} hydrocarbons was determined as the sum of C_4 hydrocarbons identified in gaseous reaction products ($\Delta[C_4^{gas}]$) and deposited on the catalyst surface ($\Delta[C_4^{surf}]$) as undesorbed oligomers. The concentration of the C_4^{surf} hydrocarbons was calculated from the integral amount of converted acetylene that did not participate in the formation of ethylene, ethane, and C_4^{gas} in an hour of reaction:

$$\Delta[C_4^{surf}] = \frac{\Delta[C_2H_2] - \Delta[C_2H_4] - \Delta[C_2H_6] - \Delta[C_4^{gas}]/2}{2}.$$

The rates of formation of ethylene ($w_{C_2H_2}$), ethane ($w_{C_2H_6}$), and C_4 hydrocarbons ($w_{C_4}^{tot}$, $w_{C_4}^{gas}$, and $w_{C_4}^{surf}$) were also calculated based on the integral amounts of reacted acetylene ($\Delta[C_2H_2]$) and the resulting ethylene ($\Delta[C_2H_4]$), ethane ($\Delta[C_2H_6]$), and C_4 hydrocarbons ($\Delta[C_4^{tot}]$, $\Delta[C_4^{gas}]$, and $\Delta[C_4^{surf}]$), respectively, in a reaction time equal to 1 h. The selectivity for ethylene, ethane, and C_4 hydrocarbons was calculated from the equation

$$S_{C_2H_4(C_2H_6, C_4)} = \frac{\Delta[C_2H_4](\Delta[C_2H_6], \Delta[C_4])}{\Delta[C_2H_2]} \times 100\%.$$

The elemental analysis of samples was performed on an Optima 2000 DN atomic emission spectrometer. The measurements were performed in solutions; for this purpose, the samples were fused with $LiBO_3$ and dissolved in HCl. The prepared samples were burned in an electric arc at 7273 K with the use of argon as a carrier gas.

The IR spectra were measured at an adsorption temperature using a Shimadzu 8300 Fourier transform spectrometer with a resolution of 4 cm^{-1}; the number of accumulated spectra was 50. The samples were pressed as pellets with a density of 7–17 mg/cm^2, calcined in an IR cell for 1 h at 723 K and a pressure of 10^{-4}–10^{-5} Torr, and cooled to 163 K with liquid nitrogen. Carbon monoxide was used as a probe molecule in order to determine the states of palladium and silver and the Lewis acid sites on the catalyst surface [11]. The adsorption of CO was performed at a liquid nitrogen temperature over the pressure range 0.1–10 Torr. The concentrations of CO complexes with palladium, silver, and the Lewis acid sites of aluminum oxide (N_{CO}) were determined from the integrated intensities of absorption bands due to the corresponding complexes of adsorbed CO normalized to pellet thickness (I_{CO}) with consideration for integral absorption coefficients (I_0) taken from [11] using the equation $N_{CO} = I_{CO}/I_0$. The integrated absorption coefficients of the Lewis acid sites of aluminum oxide, which depend on the absorption band positions of CO complexes in the range ν_{CO} = 2180–2240 cm^{-1}, were calculated from the equation $I_0 = 0.13\ (\nu_{CO} - 2130)$ [11]. The strength of Lewis acid sites was characterized by the heat of adsorption of CO (Q_{CO}), which was determined from the correlation equation [11] $Q_{CO,i} = 10.5 + 0.5\ (\nu_{CO,i} - 2143)$, where $\nu_{CO,i}$ is the vibration frequency of CO adsorbed at the ith Lewis site.

The diffraction patterns were measured on a DRON-2 diffractometer using CuK_α radiation with a monochromatic filter. The range of recording angles 2θ varied from 5° to 95°. The phase composition, unit-cell parameters, and crystallite sizes were calculated using the Material Analysis Using Diffraction special program package.

The thermal analysis of samples was performed on a Q-1500 D derivatograph (F. Paulik, J. Paulik, and L. Erdey) in a temperature range from 293 to 1273 K at a heating rate of 10 K/min in an atmosphere of air; the sample weight was ~0.2 g; the accuracy in the determination of weight losses was ±0.5 rel %.

Table 1. Concentrations of palladium and silver in initial and treated catalyst samples according to atomic emission analysis

Sample	Total element concentration, μmol/g	
	Pd	Ag
A	2.80	18.52
B	2.72	17.59
C	2.72	16.67

RESULTS AND DISCUSSION

According to atomic emission analysis data (Table 1), the total palladium content of the catalyst remained almost unchanged in the course of operation. Unlike palladium, the amount of supported silver insignificantly decreased with process duration; this can be explained by the partial carryover of the promoter with the flow of raw materials. In this case, the accumulation of catalyst poisons, such as sulfur, lead, arsenic, vanadium, antimony, and mercury, did not occur. In the spent samples, the concentrations of sodium and manganese somewhat increased from 0.31 to 0.39–0.59 and from 0.38 to 0.74–0.89 wt %, respectively; it is likely that these elements were supplied to the reactor with the flow of raw materials. The spent catalyst samples ranked only slightly below the initial catalyst in steady-state activity (Fig. 1) and acetylene conversion (Table 2). As can be seen in Tables 2 and 3, the selectivity and the rate of ethylene formation in the presence of the fresh catalyst were much higher than in the case of the spent samples. A decrease in the rate of ethylene formation in the presence of samples B and C can be due to both the hydrogenation of ethylene to ethane (Fig. 2) and the acceleration of acetylene dimerization. In this case, the effect of the dimerization reaction was less significant: the rate of formation of C_4 hydrocarbons was lower than that of ethane by one order of magnitude (Table 3). The acceleration of ethane formation from the parent or resulting ethylene can result from a change in the degree of interaction between palladium and silver atoms. Upon the promotion of a catalyst with silver [12], the partial positive charge that appears on highly dispersed palladium particles is compensated and the activity of these particles toward olefin molecules decreases.

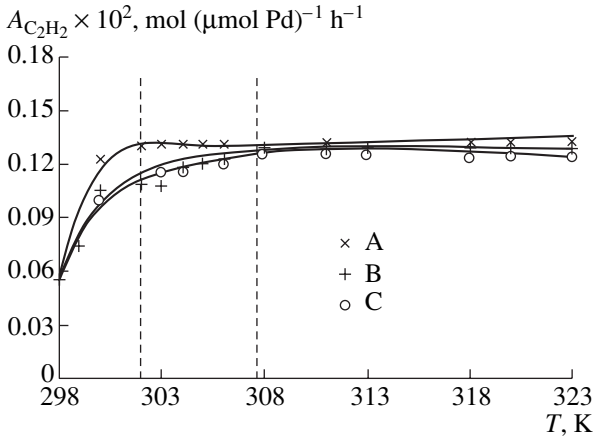

Fig. 1. Effect of temperature on the activity of catalysts A, B, and C in the reaction of selective acetylene hydrogenation.

Another distinctive feature of spent catalyst samples consists in an increase in the theoretically possible yield of C_4 hydrocarbons ($w_{C_4}^{tot}$) with the duration of operation. We calculated this yield from the amount of converted acetylene that did not participate in the formation of ethylene and ethane. A simultaneous decrease in the yield of gaseous C_4 hydrocarbons was accompanied by a considerable increase in the amount of C_4 hydrocarbons that participated in the formation of oligomeric compounds, which remained on the catalyst surface.

The states of Pd and Ag on the catalyst surface were characterized using the IR spectra of adsorbed carbon monoxide. The spectra of reduced samples (Fig. 3) did not allow one to judge changes in the properties of supported metals [13–16] because of the low concentration of palladium and the absence of the interaction of surface silver atoms with carbon monoxide molecules under experimental conditions [14]. Indirect information on the surface concentration, dispersity, and accessibility of metals to adsorbate molecules can be obtained from an analysis of the spectra of oxidized samples (Fig. 4). Note that these spectra allowed us to monitor changes in the supported metals in the course of catalyst operation, even though these spectra did not reflect the real state of supported metals under the reduction conditions of the hydrogenation reaction.

The strongly bound complexes of CO with ionic palladium and silver species were formed even at low (P = 0.1–0.4 Torr) surface coverages with the adsorbate. In Fig. 4, absorption bands at ν_{CO} = 2194–2200, 2167, and 2110–2128 cm^{-1} can be seen clearly. These absorption bands were due to the vibrations of carbon monoxide coordinated to the Lewis acid sites of aluminum oxide [11] and linear carbonyls bound to Pd^+ [15, 16] and Ag^+ ions [13, 14, 17], respectively.

In the case of samples B and C, an increase in the absorption band intensity at 2128 cm^{-1} and a broadening of this absorption band toward the low-frequency region to 2110 cm^{-1} suggest the formation of additional Pd^+ ions and CO adsorption sites related to $Pd^{\delta+}$ having an intermediate oxidation number (from 1+ to 0) [15, 16] (Table 4). This can be due to a partial charge redistribution on palladium ions, which likely occurred in the initial unreduced catalyst in two forms (Pd^+ and Pd^{2+}). The concentrations of CO complexes with Pd^+ in both of the treated samples were 3 μmol/g (Table 4), which is close to the total palladium content of the catalyst (Table 1). This allowed us to hypothesize a highly

Table 2. Acetylene conversion ($X_{C_2H_2}$), activity ($A_{C_2H_2}$), and selectivity for ethylene ($S_{C_2H_4}$) and ethane ($S_{C_2H_6}$) in the reaction of acetylene hydrogenation on catalyst samples

Sample	$X^*_{C_2H_2}$, %	$A^*_{C_2H_2} \times 10^2$, mol (μmol Pd)$^{-1}$ h^{-1}	$S^*_{C_2H_4}$, %	$S^*_{C_2H_6}$, %	$S^{*\,total}_{C_4}$, %
A	99.7	0.130	65.1	26.9	8.0
B	99.2	0.124	57.1	33.1	9.8
C	99.2	0.128	46.5	38.0	15.5

* Average values after reaching steady-state activity at T = 303–323 K.

Table 3. Rates of formation of ethylene, ethane, and C_4 hydrocarbons on catalyst samples in the reaction of selective acetylene hydrogenation

Sample	Rate of formation of C_2–C_4 hydrocarbons*, mol (μmol Pd)$^{-1}$ h^{-1}				
	$w_{C_2H_4} \times 10^2$	$w_{C_2H_6} \times 10^2$	$w^{total}_{C_4} \times 10^3$	$w^{gas}_{C_4} \times 10^3$	$w^{surface}_{C_4} \times 10^3$
A	0.085	0.035	0.049	0.043	0.006
B	0.071	0.041	0.073	0.040	0.033
C	0.059	0.048	0.081	0.035	0.046

* Average values after reaching steady-state activity at T = 303–323 K.

dispersed state of palladium particles on the catalyst surface; it is likely that this state also remained unaffected after the reduction of the samples in hydrogen.

Unlike palladium, the amount of Ag^+–CO fragments in spent samples decreased (Table 4). The intensity of absorption bands with ν_{CO} = 2167 cm^{-1} noticeably decreased as the catalyst operation time was increased; however, the position of this absorption band remained unchanged. The latter circumstance suggests that the aggregation of silver particles did not occur in the course of operation; however, the accessibility of these particles to adsorbate molecules decreased. The decrease of the Ag^+–CO/Pd^+–CO ratio allowed us to assume that the number of silver ions in the nearest environment of the palladium ion decreased. Reduction in an atmosphere of hydrogen will not have a considerable effect on the above ratios between the particles of silver and palladium accessible to adsorbate molecules. In turn, the observed changes can be reflected in the promoting effect of silver atoms and the ability of these atoms to compensate for the excessive positive charge that appeared on palladium atoms because of the effect of the strong metal–support interaction [12, 18]. It is likely that an increase in the degree of interaction of unsaturated hydrocarbons with palladium atoms caused the observed decrease in the selectivity of the process for ethylene (Table 2) and the decrease in the rate of ethane formation (Table 3).

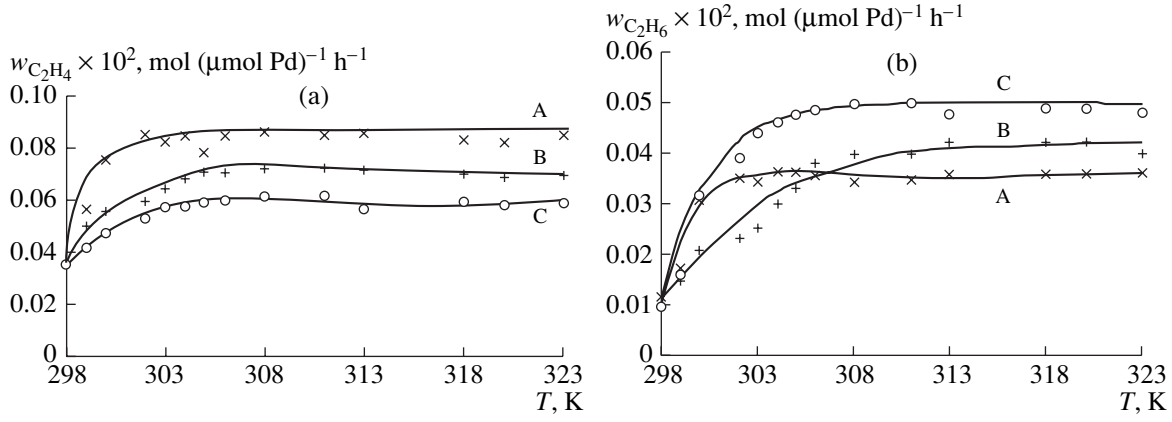

Fig. 2. Effect of temperature on the rates of formation of (a) ethylene and (b) ethane in the reaction of selective acetylene hydrogenation on catalysts A, B, and C.

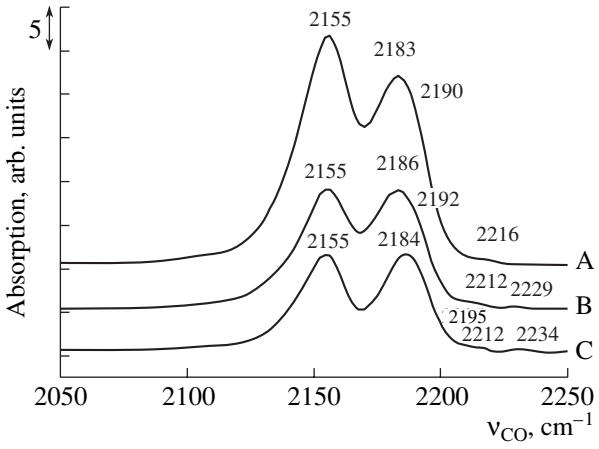

Fig. 3. IR spectra of the reduced forms of samples A, B, and C of the selective hydrogenation catalyst (P_{CO} = 10 Torr).

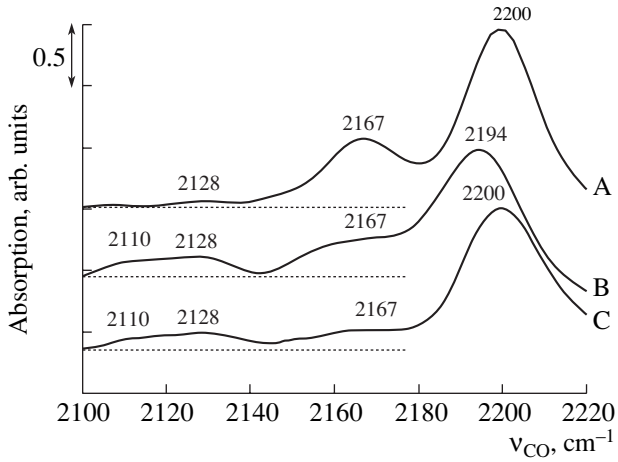

Fig. 4. IR spectra of the oxidized forms of samples A, B, and C of the selective hydrogenation catalyst (P_{CO} = 0.1 Torr).

It is likely that, in the course of catalyst operation, other reasons were responsible for the acceleration of a side process of acetylene dimerization to 1,3-butadiene [19, 20], a precursor of butenes and butane, which were identified in gaseous reaction products, as well as surface oligomers. Asplund [7] found that the amount and the rare of accumulation of hydrocarbon deposits on the surface of Pd/Al_2O_3 in the hydrogenation of acetylene largely depend on the morphology and surface area of alumina and hypothesized that the hydrocarbon chain can grow by a carbonium ion mechanism with the participation of the Lewis acid sites of the support. Moreover, Prokudina et al. [21] found that the strength of Lewis acid sites noticeably affects the carbonization of the surface of aluminum oxide.

The IR-spectroscopic study of the acid properties of the catalyst surface allowed us to recognize four types of Lewis sites (L_1–L_4) with corresponding absorption bands in the region ν_{CO} = 2183–2234 cm^{-1} in the spectra of adsorbed carbon monoxide (Table 5). The concentration (N_{CO}) and strength (Q_{CO}) of Lewis acid sites changed in the course of operation. The concentration of weak L_1 sites remained almost unchanged against the background of a decrease in the total Lewis acidity. Simultaneously, a decrease in the amount of medium-strength sites (L_2) and the appearance of additional strong (L_3) and very strong (L_4) sites were noted. In a comparison between the results of catalytic tests (Table 3) and data on the Lewis acidity, a correlation was found between the selectivity and rate of formation of C_4 hydrocarbons, which participate in the formation of oligomers deposited on the catalyst surface, and the amount of the strongest Lewis sites. The rate of formation of surface hydrocarbon deposits from acetylene dimerization products (C_4^{surf}) significantly decreased as the total concentration of L_3 and L_4 sites increased. It is believed that oligomerization processes on the catalyst surface are catalyzed by the strong Lewis acid sites of aluminum oxide with the heats of adsorption of carbon monoxide from 45 to 56 kJ/mol. It is likely that the period of operation between regenerations and its gradual shortening in the course of catalyst operation depend on the appearance of structural fragments that are responsible for strong Lewis acidity on the surface of aluminum oxide.

The acid characteristics of aluminum oxide depend on its morphology, which was studied by X-ray diffraction (XRD) analysis and thermogravimetry. Table 6 summarizes the results. According to XRD data, the starting catalyst support was γ-Al_2O_3 with a small impurity of the χ phase; γ-Al_2O_3 was inhomogeneous

Table 4. Absorption band frequencies of CO adsorbed on palladium and silver in oxidized catalyst samples

Sample	Pd^+–CO		Ag^+–CO		$\frac{Ag^+–CO}{Pd^+–CO}$, μmol/μmol
	ν_{CO}, cm^{-1}	N_{CO}, μmol/g	ν_{CO}, cm^{-1}	N_{CO}, μmol/g	
A	2128	<1	2167	20	~20.0
B	2128	3	2167	15	5.0
C	2128	3	2167	8	2.7

* The spectrum contained an absorption band with ν_{CO} = 2110 cm^{-1} ($Pd^{\delta+}$–CO).

Table 5. Surface Lewis acid sites in the samples of the selective hydrogenation catalyst

L site	A			B			C		
	ν_{CO}, cm^{-1}	Q_{CO}, kJ/mol	N_{CO}, $\mu mol/m^2$	ν_{CO}, cm^{-1}	Q_{CO}, kJ/mol	N_{CO}, $\mu mol/m^2$	ν_{CO}, cm^{-1}	Q_{CO}, kJ/mol	N_{CO}, $\mu mol/m^2$
L_1	2183	30.5	2.487	2186	32	2.154	2184	31	2.547
L_2	2190–2220	34–39	1.553	2192	35	0.465	2195–2199	36.5–38.5	0.468
L_3	2216	47	0.003	2212	45	0.018	2212	45	0.039
L_4	–	–	–	2229	53.5	0.015	2234	56	0.019
ΣL_i			4.043			2.652			3.073

Table 6. Changes in the phase composition of the support in the samples of the selective hydrogenation catalyst

Sample	Concentration, wt %					
	thermal analysis		X-ray diffraction analysis			
	Al_2O_3	boehmite	γ-Al_2O_3		χ-Al_2O_3	boehmite
			crystalline	poorly crystallized		
A	100	–	84.4	14.3	1.3	–
B	97.5	2.5	83.5	11.8	1.4	3.1
C	95.7	4.3	83.0	9.8	1.2	5.8

and consisted of well-crystallized and poorly crystallized forms. The poorly crystallized oxide cannot be related to classical amorphous aluminum oxide. The difference curve of thermal decomposition (not given in this paper) did not exhibit a characteristic exothermic effect of the phase transition of γ-Al_2O_3 via metastable alumina phases to α-Al_2O_3 around ~1073 K [22]. In the course of operation, the phase composition of the support changed. In the spent catalysts, a new compound was formed: aluminum hydroxide with the boehmite morphology (Table 6). This compound was formed because of the surface rehydration of poorly crystallized γ-Al_2O_3 in the course of regeneration under hydrothermal conditions. In this case, the DTA curves of spent samples exhibited additional endothermic effects in the temperature range 729–848 K due to the removal of interlayer water from the boehmite structure and the phase transition of boehmite to γ-Al_2O_3 [6]. As the duration of operation was increased, the endo effects shifted toward higher temperatures; this fact suggests the agglomeration of hydroxide particles and an improvement of the crystal structure [23]. The phase and structure transformations of the alumina support can cause the above decrease in the accessibility of silver particles to adsorbate molecules and change in the ratio between silver and palladium in the course of catalyst operation.

Moreover, the experimental results allowed us to attribute the weak L_1 sites with Q_{CO} = 30.5–32 kJ/mol in the catalyst to coordinatively unsaturated aluminum cations on the surface of well-crystallized γ-Al_2O_3 because, according to Paukshtis [11], only these sites occurred in γ-Al_2O_3 with a well-formed crystal structure. Paukshtis [11] interpreted L_2 sites with absorption bands in the region ν_{CO} = 2190–2200 cm^{-1} as aluminum cations in the nuclei of the Al_2O_3 phase, whereas sites with absorption bands at ν_{CO} = 2218–2230 cm^{-1} were considered as aluminum cations in Al_5–O–Al_5 clusters formed from the dimeric complexes $Al_2(OH)_6$. It is believed that, in the case under consideration, the fragments responsible for medium-strength Lewis sites with Q_{CO} = 34–39 kJ/mol are poorly crystallized γ-Al_2O_3 microcrystallites, which either are the nuclei of an aluminum oxide phase or exhibit their properties. Upon the rehydration of poorly crystallized γ-Al_2O_3, its concentration decreased to cause a decrease in the amount of the nuclei of the aluminum oxide phase and, consequently, L_2 sites. It is most likely that the simultaneous appearance of a new boehmite phase as a constituent of the support was responsible for an increase in the concentration of strong L_3 sites with Q_{CO} = 45 kJ/mol and the appearance of new, very strong L_4 sites with Q_{CO} = 53.5–56.0 kJ/mol. This can be facilitated by the formation of new crystallization bonds between primary boehmite plates, which are agglomerated under the hydrothermal conditions of steam regeneration. The noncoherent coordination [24] of primary boehmite particles along the plane [010], which is enriched in hydroxyl groups [25], can be accompanied by the formation of not only hydrogen bonds between surface OH groups but also Al–OH–Al bridging hydroxyl groups, which bind boehmite crystals to each other. The latter hypothesis was supported by a proportional increase in the concentration of the strongest (L_3 and L_4) Lewis sites upon an almost twofold increase in the boehmite content of the catalyst. Consequently, the

resulting boehmite can be a source of the strongest Lewis acid sites, which participate in the oligomerization of acetylene dimerization products and affect the deactivation of the catalyst by shortening its interregeneration cycle.

Thus, phase changes in the alumina support as a result of its rehydration were accompanied by a decrease in the accessibility of supported silver particles to a gas phase and a decrease in the amount of these particles in the nearest environment of palladium particles (which was responsible for a change in selectivity for ethylene), as well as the appearance of strong Lewis acid sites, which catalyze oligomerization processes on the catalyst surface.

REFERENCES

1. Plate, N.A. and Slivinskii, E.V., *Osnovy khimii i tekhnologii monomerov* (Fundamentals of Monomer Chemistry and Engineering), Moscow: Nauka, 2002.
2. Khrenov, E.G., Perminova, E.A., Fal'kov, I.G., et al., *Promyshlennost' sinteticheskogo kauchuka* (Synthetic Rubber Industry), Moscow: TsNIITENeftekhim, 1993, no. 2.
3. Bond, G.C., *Appl. Catal., A*, 1997, vol. 149, p. 3.
4. Duca, D., Frusteri, F., Parmalina, A., et al., *Appl. Catal., A*, 1996, vol. 146, p. 269.
5. Duca, D., Barone, G., Varga, Z., et al., *Catal. Lett.*, 2001, vol. 72, nos. 1–2, p. 17.
6. Shaikhutdinov, Sh.K., Frank, M., Baumer, M., et al., *Catal. Lett.*, 2002, vol. 80, nos. 3–4, p. 115.
7. Asplund, S., *J. Catal.*, 1996, vol. 158, p. 267.
8. Liu, R.-J., Crozier, P.A., Smith, C.M., et al., *Appl. Catal., A*, 2005, vol. 282, p. 111.
9. Ostrovskii, N.M., *Kinetika dezaktivatsii katalizatorov* (Catalyst Deactivation Kinetics), Moscow: Nauka, 2001.
10. Voronova, G.A., Vodyankina, O.V., Belousova, V.N., et al., *Kinet. Katal.*, 2003, vol. 44, no. 5, p. 713 [*Kinet. Catal.* (Engl. Transl.), vol. 44, no. 5, p. 652].
11. Paukshtis, E.A., *Infrakrasnaya spektroskopiya v geterogennom kislotno-osnovnom katalize* (Infrared Spectroscopy in Heterogeneous Acid–Base Catalysis), Novosibirsk: Nauka, 1992.
12. Huang, D.C., Chang, K.H., Pong, W.F., et al., *Catal. Lett.*, 1998, vol. 53, p. 155.
13. Muslehiddinoglu, J. and Vannice, M.A., *J. Catal*, 2003, vol. 213, p. 305.
14. Giordano, L., Del Vitto, A., Pacchioni, G., et al., *Surf. Sci.*, 2003, vol. 540, p. 63.
15. Davydov, A.A., *IK-spektroskopiya v khimii poverkhnosti okislov* (IR Spectroscopy in Oxide Surface Chemistry), Novosibirsk: Nauka, 1984.
16. Temkin, O.N. and Bruk, L.G., *Usp. Khim.*, 1983, vol. 52, no. 2, p. 206.
17. Akolekar, D.B. and Bhargava, S.K., *J. Mol. Catal.*, 2000, vol. 157, p. 199.
18. Alekseev, O.S. and Ryndin, Yu.A., *Usp. Khim.*, 1992, vol. 61, no. 4, p. 765.
19. Mornar, A., Sarkany, A., and Varga, M., *J. Mol. Catal. A: Chem.*, 2001, vol. 173, p. 185.
20. Sarkany, A., *React. Kinet. Catal. Lett.*, 2001, vol. 74, no. 2, p. 299.
21. Prokudina, N.A., Chesnokov, V.V., Paukshtis, E.A., et al., *Kinet. Katal.*, 1989, vol. 30, no. 4, p. 949.
22. Dzis'ko, V.A., Tarasova, D.V., and Karnaukhov, A.P., *Fiziko-khimicheskie osnovy sinteza okisnykh katalizatorov* (Physicochemical Foundations of the Synthesis of Oxide Catalysts), Novosibirsk: Nauka, 1978.
23. Paramzin, S.M., Zolotovskii, V.P., and Buyanov, R.A., *Sib. Khim. Zh.*, 1992, no. 2, p. 130.
24. Lamberov, A.A., Levin, O.V., Egorova, S.R., et al., *Zh. Prikl. Khim.*, 2003, vol. 76, no. 1, p. 50.
25. *Physical and Chemical Aspects of Adsorbents and Catalysts*, Linsen, B.G., Ed., London: Academic, 1970.